JOURNAL OF PHYSICAL ORGANIC CHEMISTRY
J. Phys. Org. Chem. 2006; **19:** 765–770
Published online in Wiley InterScience (www.interscience.wiley.com). DOI: 10.1002/poc.1076

Substituent effects on ion complexation of *para-tert*-butylcalix[4]arene esters†

Márcio Lazzarotto,[1]* Marjarie Marrie Francisco,[1] Francine Furtado Nachtigall[1] and Marcelo Lazzarotto[2]

[1]Departamento de Química Orgânica, UFRGS, Av. Bento Gonçalves 9500, Campus do Vale, Porto Alegre, Rio Grande do Sul, CEP 91501-970 C.P. 15003, Brasil
[2]Embrapa Uva e Vinho, R. Livramento, 515, Bento Gonçalves, RS, CEP 95.700-000, C.P. 130, Brasil

Received 18 November 2005; revised 28 December 2005; accepted 8 March 2006

ABSTRACT: Phenoxy-carboxy-methoxy-*p-tert*-butylcalix[4]arene esters were synthesized in order to evaluate the role of electronic parameters on the complexation of alkaline metal cations. Extraction constants of metal picrates to organic phase were determined. Plots of log (K_R/K_H) against Hammett σ and σ_p^+ gave good linear correlations. The best correlations with σ were obtained for K^+ and Rb^+, while the best correlations with σ_p^+ were obtained for Li^+ and Na^+. All Hammett plots gave a straight descending line, which is consistent with a dependence of the electronic density on the C═O. Treatment of data using the Yukawa–Tsuno equation revealed a variation in the contribution of resonance in the complexation of alkaline metal ions, which is maximum for Na^+ and minimum for Rb^+. Electronic parameters were calculated for a related acyclic model structure and only the HOMO energy showed a good correlation with log (K_R/K_H). Copyright © 2007 John Wiley & Sons, Ltd.

KEYWORDS: supramolecular chemistry; Hammett's correlation; calixarenes; cation complexation

INTRODUCTION

Investigations into free-energy linear relationships allow an understanding of the molecular parameters involved in dynamic chemical processes. Hammett's plot is the most useful relationship for the evaluation of the role of the electronic contribution, when sterical crowding of substituents does not greatly affect the magnitude of the constants. Host–guest chemistry usually does not fit this requirement, because complementary structures are needed for host–guest interactions and only a few studies dealing with Hammett correlations in supramolecular chemistry[1–4] have been reported, with fair success, despite the number of variables that influence the degree of complexation.

The suitability of *O*-acetyl esters of calixarenes for the extraction of alkaline metal cations is well known.[5] It has been found that calix[4]arene in cone conformation is selective for sodium, whereas the selectivity of calix[4]-arene in the 1,3 alternate conformation is shifted to potassium,[6] and calix[6]arene complexes cesium selectively.[7] The driving force for the formation of the metal-calixarene complex is the electrostatic interaction of the metal cation with the lone-pairs of the oxygen atoms. The complex formation occurs through the reorganization of the host to fit the sphere around the cation, with loss of rotational and vibrational modes of the species.[8] The structure of the sodium complex with the *O*-acetyl calix[4]arene ethyl ester has been shown to have the Na^+ cation coordinated to the eight oxygen atoms of $OCH_2C{=}O$ groups,[9] which for the uncomplexed metal-receptor span out of the center-symmetric axis of the calixarene, as non-ordered chains. The association of alkaline metals with calix[4]arene ethers brings into proximity the four arms containing the *O*-acetyl ester moiety and decreases the mobility of the $OCH_2C{=}O$ group (Scheme 1).

The hard–soft character of the groups present is another factor that determines the metal selectivity, shifting it from the sodium cation to the silver cation, when the C═O bond is replaced by a C═S bond in calix[4]arene esters.[10] The complex formation with alkali metal ions and substituted phenolic esters of carboxy–methoxy calixarene is a potential process for the application of Hammett relationships, since *para*-substituents can modulate the ability of carbonyl groups to interact by ion-dipole attraction with the metal ion.

EXPERIMENTAL

Phenol esters **3–8** were obtained from the reaction of the acid chloride **2** and the corresponding phenolates (Scheme 2). The yields were only moderate (30–60%),

**Correspondence to:* M. Lazzarotto, Departamento de Química Orgânica, UFRGS, Av. Bento Gonçalves 9500, Campus do Vale, Porto Alegre, Rio Grande do Sul, CEP 91501-970, C.P. 15003, Brasil.
E-mail: marcio@iq.ufrgs.br
†Selected article presented at the Eighth Latin American Conference on Physical Organic Chemistry (CLAFQ0–8), 9–14 October 2005, Florianopolis, Brazil.

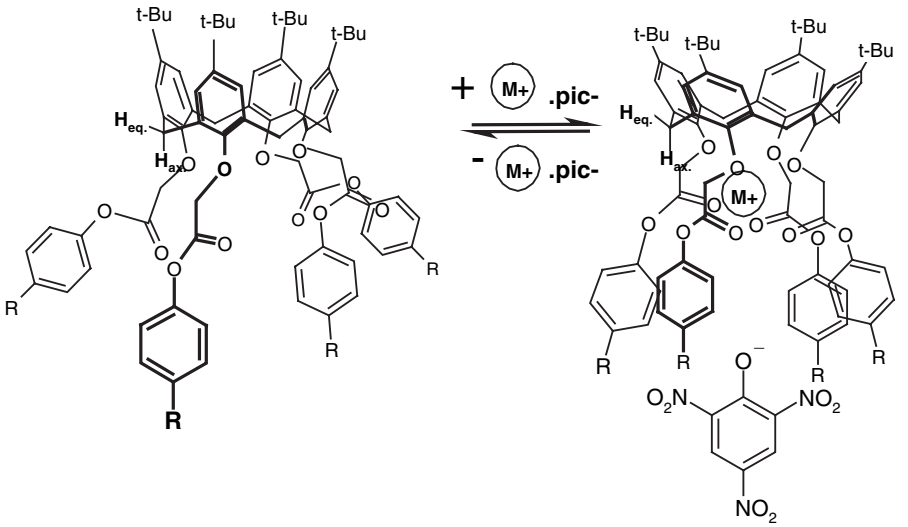

Scheme 1. Equilibrium of cation complexation

obtained through the partial substitution of the chloride during the workup process, yielding some hydrolysis products. The synthesis of **2** has been previously described[7] and the general procedure for the synthesis of the phenol derivatives **3–8** is given below. The acid chloride **2** was freshly prepared by the treatment of 200 mg (0.23 mmol) of tetrakis(hydroxy-carboxy-methoxy)-*p-tert*-butylcalix[4]arene with $SOCl_2$, and dissolved in 5 mL of dichloromethane. This solution was added dropwise to a solution of 1.80 mmol of the corresponding phenol, 230 μL (1.78 mmol) of triethylamine and 200 mg (1.78 mmol) of potassium *tert*-butoxide in 10 mL of dry acetonitrile, and the mixture was left to stand overnight under magnetic stirring. The organic phase was washed-with 0.1 mol/L NaOH and water, dried over $MgSO_4$, and evaporated under reduced pressure. With addition of methanol, the product crystallized after some minutes. Recrystallization from dichloromethane/methanol yielded the pure product.

NMR analyses were carried on Varian-200 MHz and Bruker-300 MHz spectrometers, and IR spectra were collected with a Perkin–Elmer spectrophotometer. Extraction experiments were carried in water/dichloromethane in a closed tube, stirring magnetically for 60 min after which the samples were allowed to stand overnight at 10 °C. The nitro ester **8** did not extract Li^+, Rb^+, and Cs^+ picrates. The absorbance of picrate in the organic phase was determined by spectrophotometry at 375–380 nm, and the association constants were determined considering the equilibrium below, as reported by Ungaro:[11]

$$M^+_{aq} + Pi^+_{aq} + L_{org} \rightleftharpoons [LM^+.Pi^-]_{org}$$

where M^+_{aq} and Pi^-_{aq} represent the alkali cation and picrate anion in aqueous phase and L_{org} and $[LM^+.Pi]_{org}$ are, respectively, the ligand and ligand-metal complex in dichloromethane. The equation that describes the

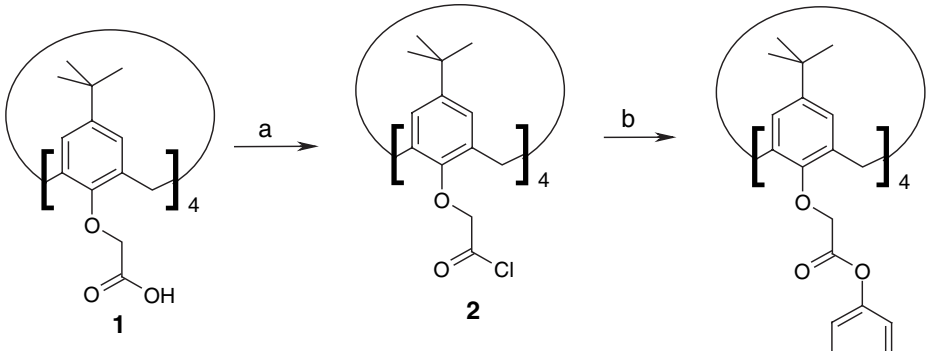

a)$SOCl_2$;b) RPhOH, *t*-BuOK, Et_3N, CH_2Cl_2

3) R= OMe; 4) R= $C(CH_3)_3$; 5) R= CH_3; 6) R= H; 7) R= Cl; 8) R= NO_2

Scheme 2. Synthesis of phenol esters from *p-t*-butyl-calix[4]arene tetraacid **1**

equilibrium is:

$$K_e = \frac{[LM^+ \cdot Pi^-_{org}]}{\gamma^2_{\pm}[M^+_{aq}][Pi^-_{aq}]\{[L_{org}]_o - [LM^+ \cdot Pi^-_{org}]\}} \quad (1)$$

where $[L_{org}]_o = [Pi^-]_o = [Pi^-_{aq}] + [Pi^-_{org}] = 1.25 \times 10^{-4}$ mol $\cdot$ L^{-1} and $[M^+_{aq}] = 1.0 \times 10^{-2}$ mol $\cdot$ L^{-1}; the activity coefficient of the ions was determined as $\gamma = 0.8$, and in order to determine $[LM^+ \cdot Pi]_{org}$, $\varepsilon_{Pi-} = 1.5 \times 10^4$ was used.

Quantum chemical calculations

The semi-empirical program package MOPAC 6.0 was used in all calculations. For each compound, computations were carried out with both the AM1[12] and the PM3[13] parameterizations. Input files were conveniently generated and before being processed the output files were visualized with RasMol 2.7.1 software. The molecular structures obtained in this way were used in a configuration interaction calculation to compute electron density on O_1, O_2, O_3, and C_1, HOMO and LUMO energies.

***p*-Methoxy-phenyl ester (3).** NMR-^{1}H ($CDCl_3$) 1.10 (s, $C(CH_3)_3$, 36 H), 3.29 (d, *J* 14 Hz, ax. $PhCH_2Ph$, 4 H), 3.76 (s, OCH_3, 12 H), 4.96 (d, *J* 14 Hz, eq. $PhCH_2Ph$, 4 H), 5.09 (s, OCH_2, 8 H), 6.74 (d, *J* 9 Hz arom. CH, 4 H), 6.83 (s, arom. CH, 8 H), 6.90 (d, *J* 9 Hz arom. C–H, 8 H); NMR ^{13}C ($CDCl_3$) 169.28, 157.00, 152.98, 145.50, 143.86, 133.46, 125.46, 122.49, 114.24, 77.76, 71.21, 55.49, 33.87, 31.92, 31.37, 30.97; elem. anal.: C = 72.41; H = 6.60, calc. for $C_{80}H_{88}O_{16}.1/3CH_2Cl_2$: C = 72.34; H = 6.70.

(3)-Na$^+$ pic$^-$. NMR-^{1}H ($CDCl_3$) 1.25 (s, $C(CH_3)_3$, 36 H), 3.49 (d, *J* 12 Hz, ax. $PhCH_2Ph$, 4 H), 3.85 (s, OCH_3, 12 H), 4.26 (d, 14 Hz, eq. $PhCH_2Ph$, 4 H), 4.67 (s, OCH_2, 8 H), 6.43 (d, *J* 9 Hz arom. C–H, 4 H), 6.73 (s, arom. CH, 8 H), 7.17 (d, *J* 9 Hz arom. C–H, 8 H).

***p-tert*-Butyl-phenyl ester (4).** NMR-^{1}H ($CDCl_3$) 1.10 (s, $C(CH_3)_3$, 36 H), 1.28 (s, $C(CH_3)_3$, 36 H), 3.30 (d, *J* 14 Hz, ax. $PhCH_2Ph$, 4 H), 4.96 (d, 14 Hz, eq. $PhCH_2Ph$, 4 H), 5.12 (s, OCH_2, 8 H), 6.83 (s, arom. CH, 8 H), 6.92 (d, *J* 9 Hz arom. C—H, 4 H), 7.26 (d, *J* 9 Hz arom. C—H, 4 H), NMR ^{13}C ($CDCl_3$): 169.24, 153.00, 148.28, 148.01, 145.47, 133.52, 126.10, 125.46, 120.98, 71.03, 34.42, 33.90, 32.03, 31.42, elem. anal.: C = 77.28; H = 7.87, calc. for $C_{92}H_{112}O_{12}.1/3CH_2Cl_2$: C = 77.11; H = 7.90.

(4)-Na$^+$ pic$^-$. NMR-^{1}H ($CDCl_3$) 1.16 (s, $C(CH_3)_3$, 36 H), 1.29 (s, $C(CH_3)_3$, 36 H), 3.52 (d, *J* 13 Hz, ax. $PhCH_2Ph$, 4 H), 4.29 (d, *J* 13 Hz, eq. $PhCH_2Ph$, 4 H), 4.70 (s, OCH_2, 8 H), 6.70 (d, *J* 9 Hz arom. C—H, 4 H), 7.17 (s, arom. CH, 8 H), 7.28 (d, *J* 9 Hz arom. C—H, 4 H).

***p*-Methyl-phenyl ester (5).** NMR-^{1}H ($CDCl_3$) NMR δ 1.10 [s, $C(CH_3)_3$, 36H), 1.63 (s, $ArCH_3$, 12 H), 3.26 [d, *J* 14 Hz, ax. $PhCH_2Ph$, 4 H), 4.80 (d, *J* 14 Hz, eq. $PhCH_2Ph$, 4 H), 5.06 (s, OCH_2, 8 H), 6.82 (s, arom. CH, 8 H), 6.86 (d, *J* 9 Hz arom. C—H, 8 H), 7.04 (d, *J* 9 Hz arom. C—H, 8 H). NMR ^{13}C ($CDCl_3$): 169.24, 153.06, 148.14, 145.74, 135.06, 133.48, 129.73, 125.46, 121.35, 76.58, 71.27, 33.86, 31.97, 31.35, 20.85; elem. anal.: C = 74.66; H = 6.99, calc. for $C_{80}H_{88}O_{12}.3/4CH_2Cl_2$: C = 74.31; H = 6.99.

Phenyl ester (6). NMR-^{1}H ($CDCl_3$) 1.11 (s, $C(CH_3)_3$, 36 H), 3.27 (d, *J* 14 Hz, ax. $PhCH_2Ph$, 4 H), 4.88 (d, *J* 14 Hz, eq. $PhCH_2Ph$, 4 H), 5.13 (s, OCH_2, 8 H), 6.84 (s, arom. CH, 8 H), 6.97 (d, *J* 9 Hz arom. C—H, 8 H), 7.15 (m, *J* 9 Hz arom. C—H, 8 H), 7.25 (d, arom. C–H, 4 H).; NMR ^{13}C ($CDCl_3$): 168.98, 152.95, 150.36, 145.58, 133.49, 129.27, 125.99, 129.57, 121.69, 71.24, 33.93, 31.63, 31.41; elem. anal.: C = 74.49; H = 6.38 calc. for $C_{76}H_{80}O_{12}.1/2CH_2Cl_2$: C = 74.83; H = 6.65.

***p*-Chloro-phenyl ester (7).** NMR-^{1}H ($CDCl_3$) 1.11 (s, $C(CH_3)_3$, 36 H), 3.27 (d, *J* 14 Hz, ax. $PhCH_2Ph$, 4 H), 4.90 (d, *J* 14 Hz, eq. $PhCH_2Ph$, 4 H), 5.08 (s, OCH_2, 8 H), 6.84 (s, arom. CH, 8 H), 6.87 (d, *J* 9 Hz arom. C—H, 8 H), 7.21 (d, *J* 9 Hz arom. C—H, 8 H). NMR ^{13}C ($CDCl_3$): 168.65, 152.71, 148.71, 145.84, 133.34, 131.10, 129.33, 125.57, 122.99, 71.04, 31.80, 31.34; elem. anal.: C = 68.86; H = 5.79, calc. for $C_{76}H_{76}Cl_4O_{12}$: C = 68.86; H = 5.38.

***p*-Nitro-ester (8).** NMR-^{1}H ($CDCl_3$) 1.12 (s, $C(CH_3)_3$, 36 H), 3.31 (d, *J* 14 Hz, ax. $PhCH_2Ph$, 4 H), 4.87 (d, *J* 14 Hz, eq. $PhCH_2Ph$, 4 H), 5.14 (s, OCH_2, 8 H), 6.86 (s, arom. CH, 8 H), 7.14 (d, *J* 9 Hz arom. C—H, 8 H), 8.11 (d, *J* 9 Hz arom. C—H, 8 H). NMR ^{13}C ($CDCl_3$): 190.07, 170.05, 168.19, 162.15, 154.76, 152.47, 125.71, 125.02, 122.35, 71.02, 31.80, 31.36; elem. anal.: C = 65.77; H = 5.61; N = 3.75 calc. for $C_{76}H_{76}N_4O_{20}.1/3CH_2Cl_2$: C = 68.86; H = 5.38; N = 4.02.

RESULTS AND DISCUSSION

Extraction data show that phenolic esters **3–8** are selective for sodium, as is known for alkyl esters of calix[4]arenes, due to the correct fit of the ionic radii with the size of the cavity.[14] The selectivity decreases as the electron withdrawing ability of the group at *para* position increases. The best receptor is compound **3**, for which the percentage extraction (%E) of Na^+ found was 85% and the selectivity expressed in terms of K_{Na^+}/K_{K^+} is 150, as reported in Table 1. Such values are not the best possible, when compared with the ethyl ester, but fall within the range of other alkyl esters.

Table 1. Percentage extraction (%E), extraction constants (K_e) and selectivity factors (K_{Na}/K_M) in extraction equilibria of alkali metal picrates from H_2O to CH_2Cl_2 in the presence of compound **3**

Metal ion	%E	K_e ($\times 10^{-5}\,M^{-2}$)	K_{Na}/K_M
Li^+	12	1.87	265
Na^+	85	497	
K^+	18	3.26	152
Rb^+	11	1.80	275
Cs^+	7	1.07	463

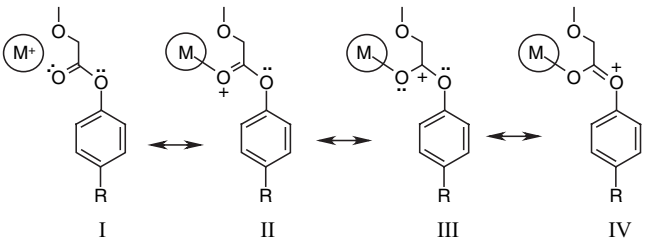

Scheme 3. Resonance structures of the metal complex

Plots of log (K_R/K_H) with σ and σ^+ parameters, showed straight lines with negative slopes for all metals, and the values of ρ are listed in Table 2. The plots using these Hammett parameters are useful to gain an understanding of the degree of electronic contribution of the *para*-group to the positive charge of the metal cation (Figs. 1 and 2).

The quality of the fittings, measured by the correlation factor *r*, for Li^+ and Na^+ and Cs^+ were better using σ_p^+, whereas for K^+ and Rb^+ the correlations were better using the parameter σ. The best correlations with σ^+ for Li^+ and Na^+ indicate that the *para*-group acts through resonance with a positive charge in these cases. This suggests a significant contribution of the mesomeric form IV (Scheme 3) for Li^+ and Na^+ complexes, where there is a significant electronic interaction between the ion and the *n* and π electrons of the ligand, with a partial development of positive charge located on the oxygen directly linked to the aromatic ring.

The Yukawa–Tsuno equation[15] allows a numeric evaluation of the contribution of resonance of the *para* group, expressed in terms of factor r_{YT}. Values of r_{YT} and ρ are reported in Table 3. The values of $r_{YT} > 1$ found for Na^+ and Li^+ show that even σ^+ underestimates the contribution of resonance on complexation. It becomes less important for K^+ and Cs^+, while the complexation of Rb^+ correlates only to σ.

$$\log \frac{K}{K_H} = \rho[\sigma + r_{YT}(\sigma^+ - \sigma)] \qquad (2)$$

Semi-empirical calculations of parameters that could be related to the complexation, for example, electron density on O_1, O_2, O_3 and C_1, HOMO and LUMO energies, were obtained using AM1 and PM3 Hamiltonians, using the structure shown in Scheme 4 as a model, in *syn*-like and *anti*-like conformations.

Initially, plots of log (K_R/K_H) with the electronic parameters were constructed for the Na^+ ion, which showed the highest variation among the values of log (K_R/K_H) and, thus, is more sensitive to the variation of the structure, and the results of the correlations are listed in Table 4. The HOMO (n C═O) energies exhibit fair to good correlations for both AM1 and PM3 Hamiltonians, the best result being obtained using AM1 on the *anti* conformer. The HOMO parameter was therefore chosen for the plots of log (K_R/K_H) for all metals, and the

Table 2. Values of the slopes (ρ) and correlation factors (*r*) for the plots of log (K_R/K_H) *versus* σ^+ and σ for the extraction experiments

	Li^+	Na^+	K^+	Rb^+	Cs^+
$\rho^+(\sigma_p^+)$	−0.60	−1.63	−1.09	−0.40	−0.39
$r^+(\sigma_p^+)$	**0.97**	**0.98**	0.95	0.84	**0.98**
ρ (σ)	−0.90	−1.96	−1.49	−0.81	−0.64
r (σ)	0.84	0.89	**0.99**	**0.97**	0.92

Table 3. Values of r_{YT} and ρ obtained through the Yukawa-Tsuno equation

	Li^+	Na^+	K^+	Rb^+	Cs^+
r_{YT}	1.3	1.9	0.2	0.0	0.7
ρ	−0.52	−1.31	−1.06	−0.81	−0.46

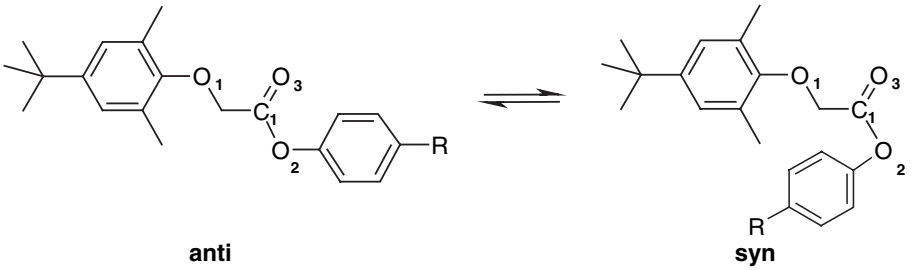

Scheme 4. Model structures for the calculation of electronic parameters

Table 4. Angular coefficients, standard deviations (SD) and correlation factors (*r*) for the plot of log $(K_R/K_H)_{Na+}$ *versus* different electronic parameters

Parameter	Angular coefficients	SD	*r*
Electron density O_1	13.45	1.17	0.05
Electron density O_2	56.55	1.09	0.36
Electron density O_3	−41.71	1.11	0.30
Electron density C_1	7.13	1.16	0.07
HOMO	4.71	0.18	0.98
LUMO	1.28	0.97	0.56

correlation factors are listed in Table 5. It is worth noting that σ^+ is linearly correlated to E_{HOMO}. Thus, the substituent effect by resonance may account for the increase in HOMO energy, which allows a more effective interaction with the electrophile.

There is a clear inversion of the best correlation for the plot of log (K_R/K_H) against HOMO-energy going from the small (Li^+, Na^+) to the larger (Rb^+, Cs^+) cations. An example is the plot of log (K_R/K_H) *versus* E_{HOMO} for the Cs^+ ion shown in Fig. 3. For Li^+ and Na^+ the best correlation was obtained for AM1-HOMO-*anti*, while for Rb^+ and Cs^+ the best correlation was obtained for AM1-HOMO-*syn*. This is indicative of the change in the conformation of the host to accommodate larger cations by an opening of the way for the binding site formed by the $OCH_2C{=}O$ group.

The ^{1}H-NMR spectra of Na^+-complexes with methoxy **3** and *t*-butyl **4** derivatives are consistent with an oxygen-bonded complex in the lower-rim. Some selected values of δ are reported in Table 6. The complexation leads to a freezing of the motion of the pendant groups, with an increase in symmetry to C_{4v}.[16] The complexation opens the *t*-butyl groups (upper-rim) and brings the phenolic oxygen atoms closer (lower-rim). The most evident change is the proximity of the doublets of the equatorial and axial methylenic hydrogen atoms. The δ values change from 5.00 and 3.27 ppm for the uncomplexed calixarene to 4.27 and 3.52 ppm for the Na^+ complex of *t*-butyl derivative **4**, as a result of the motion of the oxygen atoms linked to the calix cavity. The proximity of the axial hydrogens to the oxygen atoms in the free host is responsible for their low-field absorption and the interaction with the metal increases the distance between these oxygen atoms and the axial hydrogen atoms, so the net result is a high-field shift. The same pattern for the chemical shifts of the methylenic hydrogen atoms is observed for the complexation by the methoxy derivative **3**, indicating that the nature of the complexation is the same for both. The signals related to OCH_2 hydrogens were also shifted to a higher field: from 5.00 to 4.67 ppm

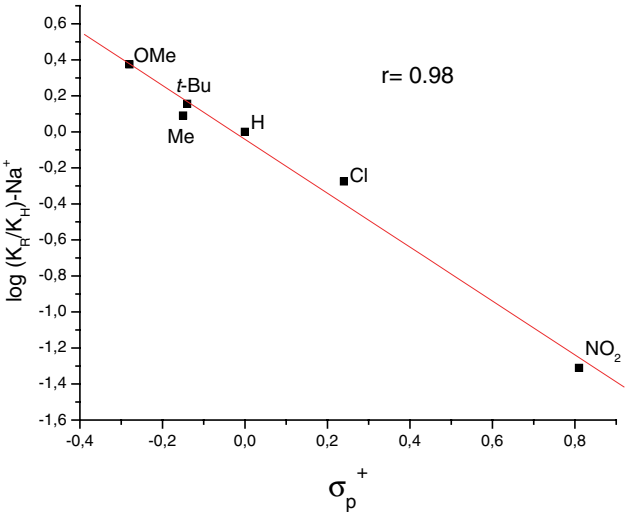

Figure 1. Hammett's plot (log K_R/K_H *vs.* σ_p^+) for extraction data of sodium picrate

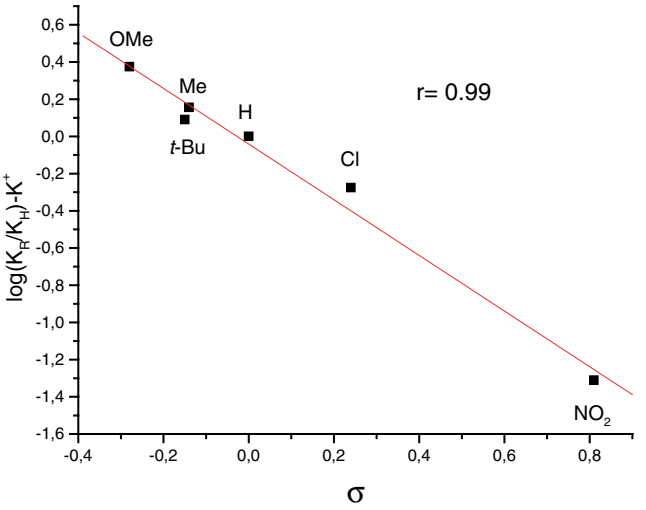

Figure 2. Hammett's plot (log K_R/K_H *vs.* σ) for extraction data of potassium picrate

Table 5. Correlation factors for the plots of log (K_R/K_H) with HOMO energies of *anti* and *syn* conformations of the model structures for calixarene receptors

	AM1-HOMO-*anti*	PM3-HOMO-*anti*	AM1-HOMO-*syn*	PM3-HOMO-*syn*
Li^+	0.92	0.11	0.90	0.81
Na^+	0.98	0.63	0.92	0.95
K^+	0.92	0.64	0.81	0.88
Rb^+	0.68	0.33	0.79	0.61
Cs^+	0.93	0.02	0.98	0.89

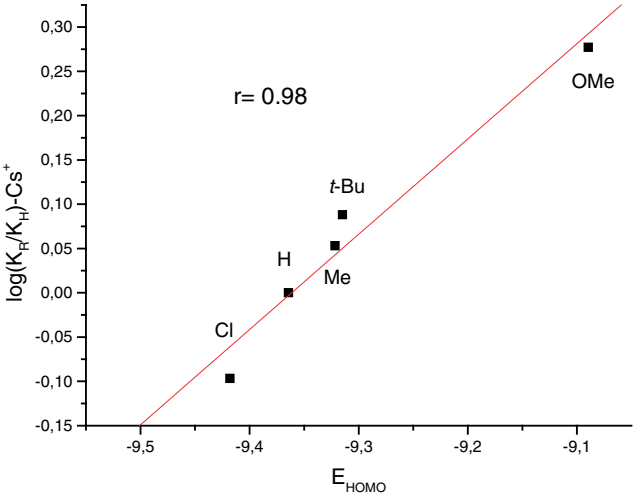

Figure 3. Plot of log (K_R/K_H) *versus* E_{HOMO} of *syn* conformation for extraction constants of cesium picrate

Table 6. Selected δ of free calixarene esters **3** and **4** and complexed with Na^+

	OMe-**3**	OMe.Na^+;-**3**.Na^+	*t*-Bu-**4**	*t*-Bu.Na^+-**4**.Na^+
$H_{ax.}$ (d)	3.29	3.49	3.30	3.52
$H_{eq.}$ (d)	4.96	4.26	4.96	4.29
OCH_2 (s)	5.09	4.67	5.12	4.70
$H_{arom.}$(s)	6.74	7.17	6.83	7.17
$H_{ortho\text{-}R}$ (d)	6.90	6.43	6.92	6.70
$H_{meta\text{-}R}$ (d)	6.83	6.73	7.26	7.28

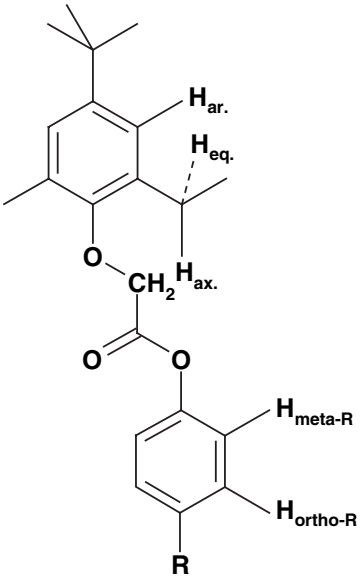

for OMe derivative-**3** and from 5.12 to 4.70 ppm for *t*-butyl derivative **4**. We conclude that the conformational change again had a considerable influence on the chemical shifts of the hosts.

However, we noticed some unexpected trends in the chemical shifts with the complexation. In the Na^+ complexes with **3** and **4**, there were shifts of the peaks corresponding to C—H at *ortho* position to the phenol esters to higher fields, when compared with the free host, while we would expect a lower field shift due to the draining of electronic density by the phenolic oxygen. We attributed this effect to a shielding of these aromatic hydrogen atoms by the pendant aromatic rings, which are brought nearer by the conformational change promoted by the metal cation complexation. This is a further indication of the *anti* conformation around the C—O bond of the ester for the Na^+ complex, when the proximity between the aromatic rings places the hydrogen atoms in the shielding region of the aromatic π-clouds.

CONCLUSIONS

Hammett plots for constants of alkaline metal extraction by *para*-substituted-phenoxy-ester-calixarenes **3–8** showed good correlations and revealed that electronic parameters can play a major role in the magnitude of the constants and improve the selectivity of metal extraction. The good correlations with HOMO energies of the host suggest that the frontier orbital interactions contribute to the complex formation.

Acknowledgements

PROSET and CNPq for financial support.

REFERENCES

1. Ungaro R, El Haj B, Smid J. *J. Am. Chem. Soc*. 1976; **98**: 5198–5202.
2. Ashton PR, Fyfe MCT, Hickingbottom SK, Stoddart JF, White AJP, Williams DJ. *J. Chem. Soc. Perkin Trans. 2* 1998; 2117–2128.
3. Carver FJ, Hunter CA, Seward EM. *Chem. Comm* 1998; 775–776.
4. Haino T, Nakamura M, Kato N, Hiraoka M, Fukazawa Y. *Tetrahedron Lett*. 2004; **45**: 2281–2284.
5. Casnati A, Sansone F, Ungaro R. *Adv. Supramol. Chem*. 2003; **6**: 165–218.
6. Iwamoto K, Shinkai S. *J. Org. Chem*. 1992; **57**: 7066–7073.
7. Arnaud-Neu F, Collins EM, Deasy M, Ferguson G, Harris SJ, Kaitner B, Lough AJ, McKervey MA, Marques E, Ruhl BL, Schwing-Weill MJ, Seward EM. *J. Am. Chem. Soc*. 1989; **111**: 8681–8691.
8. Schwing-Weill MJ, Arnaud-Neu F, McKervey MA. *J. Phys. Org. Chem* 1992; **5**: 496–501.
9. de Namor AFD, Pugliese MA, Casal AR, Aparicio-Aragon WB, Piro OE, Castellano EE. *Phys. Chem. Chem. Phys*. 2004; **6**: 3286–3291.
10. O'Connor KM, Svehla G, Harris SJ, McKervey MA. *Talanta* 1992; **39**: 1549–1554.
11. Arduini A, Pochini A, Reverberi S, Ungaro R, Andreetti GD, Ugozzoli F. *Tetrahedron* 1986; **42**: 2089–2100.
12. Dewar MJS, Zoebisch EG, Healy EF, Stewart JJP. *J. Am. Chem. Soc*. 1985; **107**: 3902–3909.
13. Stewart JJP. *J. Comput. Chem* 1989; **10**: 209–220.
14. Arduini A, Pochini A, Reverberi S, Ungaro R. *Chem. Commun*. 1984; 981–982.
15. Yukawa Y, Tsuno Y. *Bull. Chem. Soc. Jpn*. 1959; **32**: 971–981.
16. Yamada A, Murase T, Kikukawa K, Arimura T, Shinkai S. *J. Chem. Soc. Perkin Trans. 2* 1991; 793–797.